# Study and Analysis of Power Electronic Converter Circuits and Wave-forms in a Series-Series Compensated Wireless Power Transfer for Charging Electric Vehicle Batteries using MATLAB Simulink

• Kofi Addo Annan

## I. ABSTRACT

For the past two decades, the world has experienced a paradigm shift towards renewable sources of energy such as the solar power, wind, and the hydro power. Our pursuit for cleaner energies is the major reason electric vehicles are being fully realized on our roads today. For another reason, electric vehicles are more efficient than the conventional combustion engine cars. Electric vehicles on our roads today have three charging modes; conductive charging (AC/DC), wireless charging and battery swap. All these methods are realizable but have their advantages and disadvantages. Wireless charging of electric vehicles stands out in terms of efficiency, charging time, reliability, low volume, reduced cost and weight. Again, with the major deployment of autonomous driving of electric vehicles, robot taxis will be realizable within the next 3 to 5 years. The only charging mode that can be thought of when the taxis are to take power snacks is the wireless charging mode. The main purpose of this paper is to review the power electronic circuitry of the wireless chargers which consists of several power converter types and their voltage waveforms at each conversion stage. The series-series compensation topology is employed in this study.

## II. INTRODUCTION

Major playmakers in producing electric vehicle wireless charger are the WiTricity (Based in the US) and ZTE Corporation (Based in China). The wireless power transfer system has a structure that consists of two electrically insulated and separated sections. Namely; transmitter and receiver. Usually the transmitter part of the circuit is buried into the pavements. Here, most of the applicable deployment areas includes residential garages and office/shopping parking lots to achieve a static wireless charging. Another applicable deployment area is the traffic lights, bus stops and taxi ranks (taxis in queues) to achieve quasi-dynamic wireless charging and lastly, the dynamic wireless charging of electric vehicle is achievable when the transmitter component of the system is installed on the roads to provide constant charging of the electric vehicles for longer driving range and reduced volume of the battery which translates to reduced weight and hence increased efficiency of the vehicles [1]. The transmitter circuit is offered AC power from the grid (mains of the charging system) and this power is fed to the receiver circuit which is entrenched at the under part of the electric vehicle. This power is delivered to charge the EV batteries after the battery management system has communicated the charging requirements of the battery in terms of voltage and current levels. The power electronic converter circuits of the transmitter section of the wireless power transfer system comprises of a front-end AC DC power converter (Power Factor Correction rectifier). The PFC rectifier is cascaded by a high frequency inverter that feeds the transmitting device being a coupled transformer with alternating voltage and currents. Through magnetic resonance wireless power transfer which builds upon the history of inductive charging, the alternating current through the coupled transformer coil at the transmitting section creates a circular magnetic field around the coil. Thus the alternating voltage at the transmitting section induces a terminal voltage to the receiver coil at same and high frequencies between 10 kHz and 150 kHz. In this case study, both the transmitter and receiver coils are made efficient resonators and operate and tuned to the same frequency of say 41 kHz. A high frequency rectifier is employed to convert the accumulated AC power to DC. The HF rectifier is cascaded by a DC-DC converter (in-cascade chopper) which controls the voltage and

current used to charge the battery pack according to the pack charging profile and requirements. Figure 1.0 is a block diagram which describes the process above.

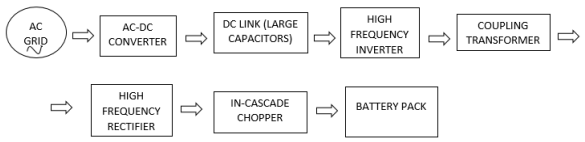


Fig. 1: Block diagram representing the charging process

## III. GENERIC ELECTRIC VEHICLE WIRELESS CHARGING ARCHITECTURE

*AC Grid*

The present world depends on electricity. Electricity is a vital resource particularly in metropolitan areas providing public security, safety and well-being. Electricity can be created, stored and used in later time. Also, the instant its produced it can be used. The infrastructure that makes this possible is the AC power grid. Basically, the power grid can be thought of a wide area interconnection between the generation, transmission and distribution stations offering severe advantages in exchange for complexity. In electric vehicle charging, the charging stations depend on the grid for AC power just like plugging in our phones and other electronics in our homes. In the same vein, wireless charging of electric vehicles depends on the AC power grid for charging. Typically, three-phase power is delivered at different three-phase voltages and frequency values at different regions or countries around the world. Basically, a three-phase voltage of either 400/415V at frequencies of either 50/60Hz.

*AC-DC Converter*

The AC-DC converter employs diodes as the rectifying components in its simplest form. The advantage of this design is;

- It is cheap.
- It is simple to setup.
- The design can be realized in both single and three phase topologies.

The disadvantage however is that for single phase topologies, the currents drawn from the AC grid are highly distorted. The remedy of this problem involves the deployment of power factor correction (PFC) circuits to control the currents drawn from the power grid and put it nearly in-phase with the voltage, and also regulate the output voltage of the AC-DC rectifier at the same time [2].

For the three phase topologies, the AC-DC converter employs active rectifier circuits. In this case, an inductor is connected in series with the power grid and MOSFETS are employed. The major advantage of this design is;

- The current now becomes pure sinusoidal thus no harmonics are observed.
- Unity power factor can be achieved.
- Losses are minimum thus higher efficiency is achieved.

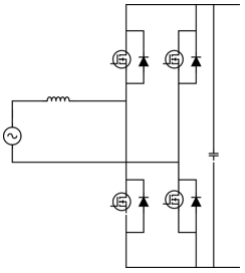

Fig. 2: Active Rectifier Circuit

*High Frequency Inverter*

The power goes into the inverter from the large capacitors (dc link). The inverter is there to create high frequency AC voltage of frequencies ranging from 10 kHz and 150 kHz.

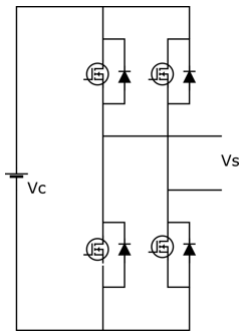


Fig. 3: Full Bridge Inverter Circuit

Contemporary wireless power transfer systems make use of voltage-fed, full-bridge resonant topologies, with the help of modern wide band gap (WBG) switches such as SiCMOSFET and SiCIGBT switches [2]. SiC gives numerous benefits as a semiconductor material over conventional Si. The SiC allow to develop a high capacity, low loss power transistor devices. The SiC devices have the advantages like;

- High efficiency

- High operating frequency and wide range of operating temperature.
- High power handling capabilities.

*Resonant Circuit Topologies for Wireless Power Transfer Systems*

As a result of the distance between the transmitting and receiver coils of the wireless power transfer system, the mutual inductance and coupling coefficient gets affected. Thus, creates a mutual inductance and large leakage inductance as well. The power transfer capability of the transmitter and receiver coils is limited as a result. The remedy of this problem demands for the need to compensate the leakage inductance in order to obtain higher mutual inductance. The circuit therefore functions at resonance frequency. In order to achieve maximum energy transfer, the coil inductance is compensated by connecting either connecting capacitor in series or parallel to the transmitting coil (primary side) and receiver coil (secondary side) thus made as active resonators tuned to resonate at the same supply frequency. According to literature, there are four fundamental resonant wireless power transfer topologies [3] ;

- Series-Series (SS)
- Series-Parallel (SP)
- Parallel-Parallel (PP)
- Parallel-Series (PS)

Others are;

- Series Parallel-Series
- LLC topology

For the purpose of this study, the SS resonant circuit topology is employed in the methodology.

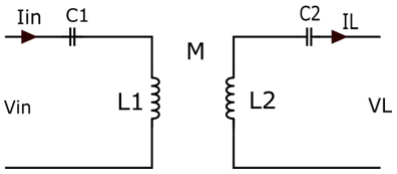


Fig. 4: Series-Series

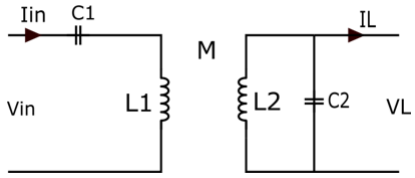


Fig. 5: Series-Parallel

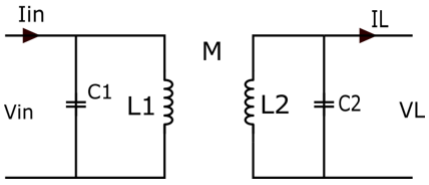


Fig. 6: Parallel-Parallel

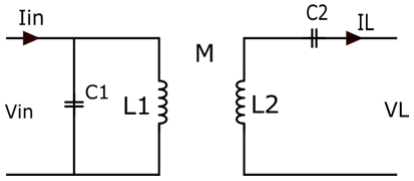


Fig. 7: Parallel-Series

## IV. METHODOLOGY

In this study, a wireless power transfer system is implemented using MATLAB Simulink software to charge a lithium ion battery. Circuit diagrams were drawn using Inkscape. Components involved include an AC power source, diodes, MOSFETs, pulse generator, mutual inductance, a voltage measurement block, inductor, scope, capacitor, and a battery.

*Series-Series resonant circuit topology*

In modeling the wireless power transfer system for this study, the SS compensation topology shown in fig.4 was used. The capacitors C1 and C2 were both connected in series to the mutual inductance at the transmitter and receiver sections respectively. This connection is used to lessen the reactive power drawn from the system and makes the resonant frequency independent of the load demand and the magnetic coupling. This topology also ensures the secondary induced current is not dependent on the load [4].

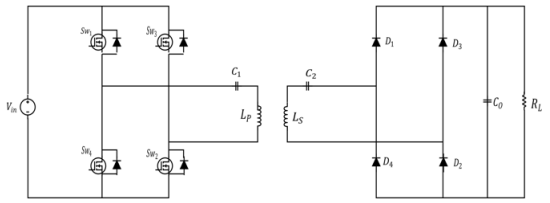

Fig. 8: a configuration showing series-series compensation in wireless power transfer circuit.

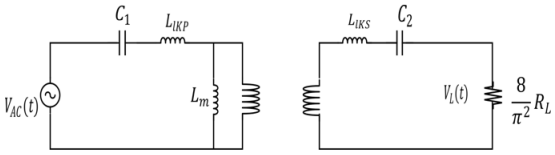

Fig. 9: shows the equivalent circuit of the SS topology.

**Comments**

- The input voltage source is connected to the full-bridge inverter circuit which applies a seemly square wave voltage $V_{AC}$ to the resonant tank circuit.
- $L_{lKP}$ and $L_{lKS}$ represents the linear transformers leakage inductance on the primary and secondary side respectively. $L_m$ is the transformer mutual inductance.
- With the exception of the fundamental harmonic component, the resonant tank circuit with the SS capacitors functions as a band pass filter, neglecting any harmonics of $V_{AC}$
- The components that makes up the secondary side, that is, the full-bridge rectifier and the capacitor acting as a filter can be represented as a load resistance$R_L$. Also, since the fundamental harmonic component of $V_{AC}$ is only accepted at the input, the load can be modelled as an AC load [5].

*Simulation results and discussion*

The parameters that describe the various components in the simulation are tabulated. Also, the scope readings of the AC-DC converter (diode rectifier) output, the high frequency inverter output, high frequency rectifier output are read and discussed. The state-of-charge (SOC), voltage (V) and current (C) of the lithium ion battery are read and discussed in this section.

**Parameters of Components**

| | |
|---|---|
| Peak Amplitude (V) | 240 |
| Phase (°) | 0 |
| Frequency (Hz) | 50 |

TABLE I: Parameters for AC Voltage Source (Power Grid)

| | |
|---|---|
| Resistance Ron ($\omega$) | 0.001 |
| Forward Voltage Vf (V) | 0.8 |
| Snubber Resistance Rs ($\omega$) | 500 |
| Snubber Capacitance Cs (F) | 250e-9 |

TABLE II: Parameters of diode in parallel with a series RC snubber circuit for rectification

| Branch Type | Capacitance (C) |
|---|---|
| Capacitance (F) | 1000e-6 |

TABLE III: Parameters of series RLC branch used as a dc link output to the rectifier

| | |
|---|---|
| Amplitude | 1 |
| Period (Secs) | 0.02 |
| Pulse width (% of period) | 50 |
| Phase Delay (Secs) | 0 |

TABLE IV: The pulse generator characteristics for MOSFET switches 1 and 2

| | |
|---|---|
| Amplitude | 1 |
| Period (Secs) | 0.02 |
| Pulse width (% of period) | 50 |
| Phase Delay (Secs) | 0.01 |

TABLE V: The pulse generator characteristics for MOSFET switches 3 and 4

| | |
|---|---|
| FET Resistance Ron ($\omega$) | 0.1 |
| Internal Diode Resistance Rd ($\omega$) | 0.01 |
| Internal Diode Forward Voltage Vf (V) | 0 |
| Snubber Resistance Rs ($\omega$) | 1e5 |
| Snubber Capacitance Cs ($\omega$) | inf |

TABLE VI: Parameters for the MOSFETs for the high frequency inverter

| Branch Type | Capacitance (C) |
|---|---|
| Capacitance (F) | 4.9e-6 |

TABLE VII: The parameters of series capacitor to both the primary and secondary sides of the transformer.

| | |
|---|---|
| Winding 1 Parameters [R1 (ohm) L1 (H)] | 0.0714 73.43e-06 |
| Winding 2 Parameters [R1 (ohm) L1 (H)] | 0.0714 73.43e-06 |
| Mutual Impedance [Rm (ohm) Lm (H)] | 0.142 1.46e-05 |

TABLE VIII: shows the parameters of mutual inductance

| Branch Type | Capacitance (C) |
|---|---|
| Capacitance (F) | 1000e-6 |

TABLE IX: Parameters of capacitor at the high frequency rectifier output.

| | |
|---|---|
| Amplitude | 1 |
| Period (Secs) | 0.02 |
| Pulse width (% of period) | 50 |
| Phase Delay (Secs) | 0 |

TABLE X: The pulse generator characteristics for MOSFET switch used in the buck converter.

| Branch Type | Inductance (L) |
|---|---|
| Inductance (H) | 750e-3 |

TABLE XI: The parameters of inductor used in the buck converter.

| Branch Type | Capacitance (C) |
|---|---|
| Capacitance (F) | 100e-6 |

TABLE XII: The parameters of capacitor used in the buck converter.

| Battery Type | Lithium-Ion |
|---|---|
| Nominal Voltage (V) | 3 |
| Rated Capacity (Ah) | 2.2 |
| Initial state-of-charge (%) | 80 |
| Battery Response time (secs) | 30 |

TABLE XIII: The battery parameters.

## Scope Output

*AC-DC Converter (Diode rectifier circuit) Output Voltage Waveform*

In a typical Ghanaian setting, a 240VAC, 50Hz will be received from the power grid at the charging point either in a home parking garage or an office parking lot. While the input of the wireless charging system is made of an AC-DC rectifying circuit, 240VAC will be transformed into a pulsating DC voltage. The simulation below shows the output waveforms;

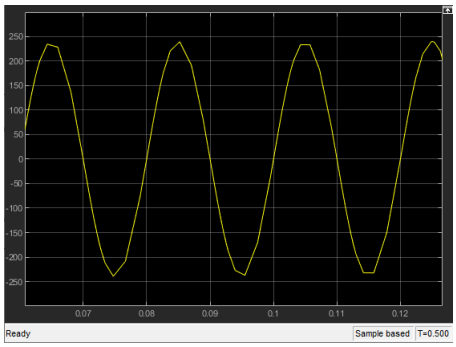


Fig. 10: shows the AC Grid Voltage

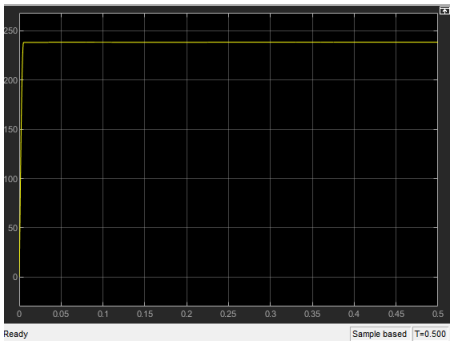


Fig. 11: shows the AC voltage rectified by the diodes

*High Frequency Inverter Output Voltage Waveform*

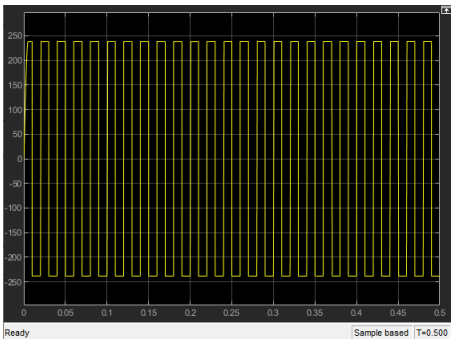


Fig. 12: High Frequency Inverter Output 1

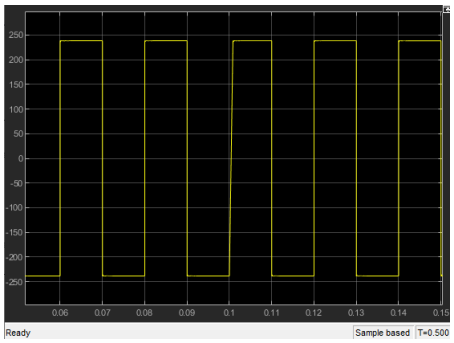


Fig. 13: High Frequency Inverter Output 2

*Observations*

It is seen that the DC power is converted to AC with a maximum value around 240 V and minimum value of about -240 V. The peak-to-peak voltage is about 480 V.

*Secondary Coil Output Voltage Waveform*

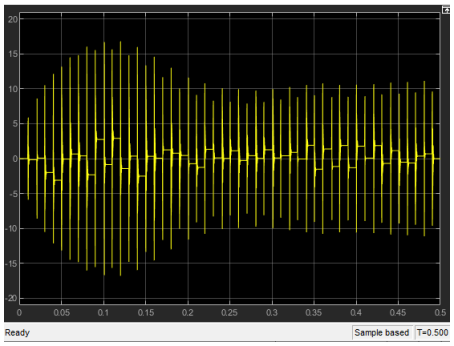


Fig. 14: Secondary Coil Output 1

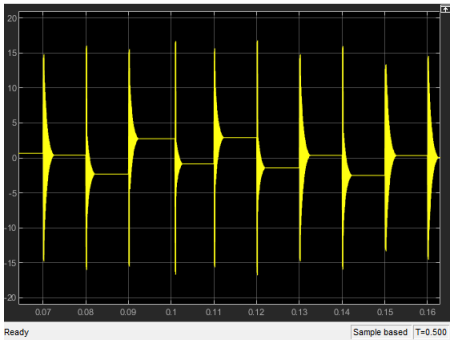


Fig. 15: Secondary Coil Output 2

*Observations*

The voltage transmitted to the secondary coil is seen to be around 15V, -15V.

*High Frequency Rectifier Output Voltage Waveform*

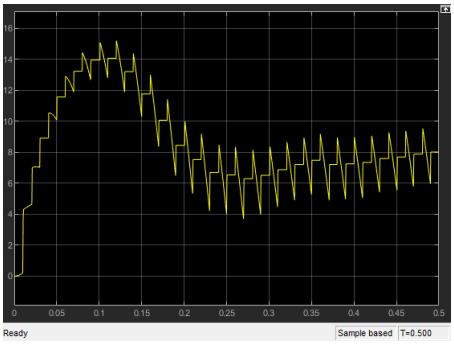


Fig. 16: High Frequency Rectifier Output 1

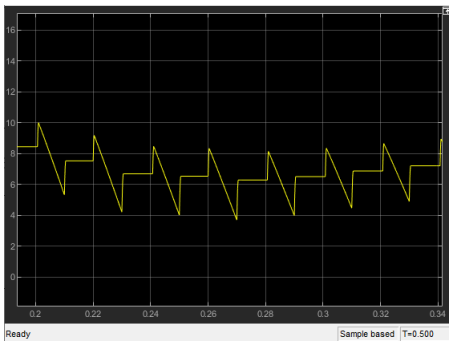


Fig. 17: High Frequency Rectifier Output 2

*Observations*

The rectified AC voltage is seen to be around an average value of 7V.

*Output Voltage Waveform of DC-DC Buck converter*

The DC voltage after the high frequency rectification is required to be further stepped-down to a voltage suitable for the battery pack.

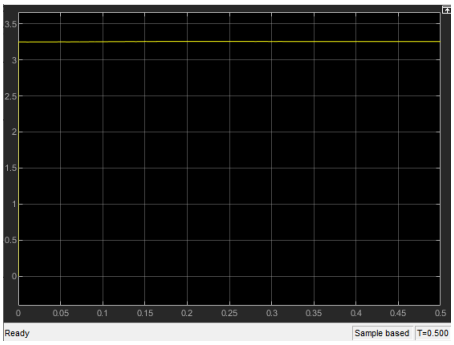


Fig. 18: DC-DC Buck converter Output

*Observations*

It is seen that there is no ripple observed at the output of the step-down chopper. Then again, it can be concluded that, the ripple is largely dependent on the value of the capacitor. The average value is seen to be around 3.3V. This makes sense following the principle;

$$\text{Duty Cycle(d)} = \frac{OutputVoltage(Vout)}{InputVoltage(Vin)}$$

The output voltage of the high frequency rectifier was 7V and the duty cycle of the pulse generator to the MOSFET was 50%.

*Lithium-Ion Battery Signals (State-of-charge SOC, Voltage and Current)*

The lithium ion battery parameters shows 3V nominal voltage, 2.2Ah rated capacity, at an initial state of charge of 80% and response time being 30s. The market of electric vehicles is trending towards fast charge. Thus the C-Rate of the lithium-ion battery is every importance factor to consider. The simulation results shows a charging current (I) of 0.3712 A. Thus the C-rate can be calculated as;

$$\text{C-Rate} = \frac{BatteryCapacity(Ah)}{ChargingCurrent(A)}$$

$$\text{C Rate} = \frac{2.2Ah}{0.3712A}$$

C-Rate = 5.93C.

The battery has a moderate fast C-rate of approximately 6C. This implies that it takes about $\frac{1}{6}$th of an hour to fill up the battery to its full capacity.

*State-of-charge (SOC)*

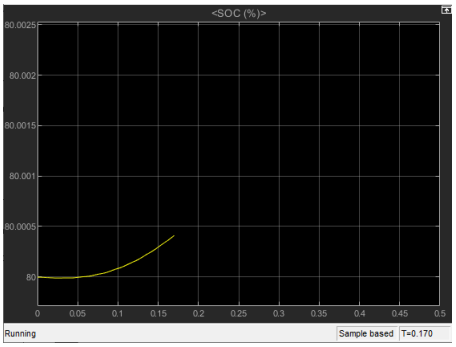


Fig. 19: Battery State of Charge at 1.17 seconds

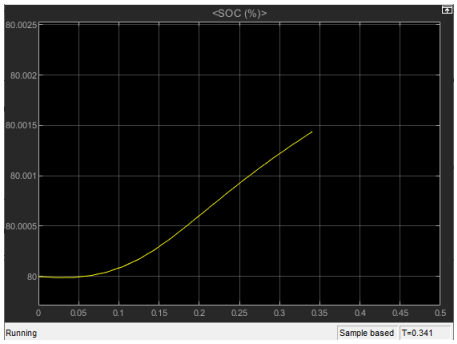


Fig. 20: Battery State of Charge at 0.34 seconds

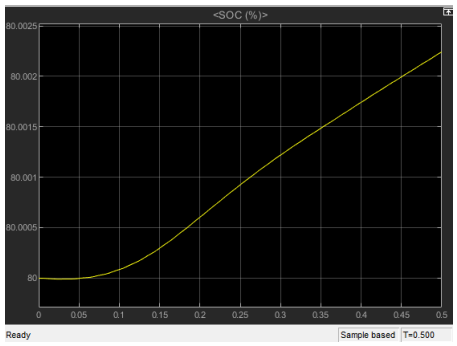


Fig. 21: Battery State of Charge at 0.5 seconds

*Observations*

The simulation shows that the SOC of the battery increases with time.

*Battery Voltage*

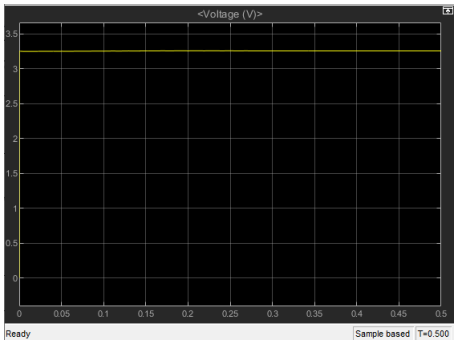


Fig. 22: Battery Voltage

*Observations*

It is observed that the battery voltage remains fairly constant.

*Battery Current*

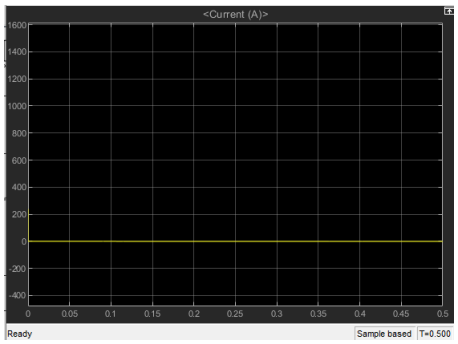


Fig. 23: Battery Current

*Observations*

The battery current output shows a no amperage. The current drops due to saturation and the battery is near fully charged.

**Measurement Table**

| | |
|---|---|
| Supply Voltage (Grid) | 240 VAC, 50 Hz |
| Output Voltage at Rectifier | 238 V, DC |
| Input Voltage to HF Inverter | 238 V, DC |
| Output Voltage of HF Inverter | 238 V, -238 V, 476 VAC pk-pk |
| Voltage of the Secondary Coil | 15V, -15V AC |
| Output Voltage of HF Rectifier | 6V, DC |
| Output Voltage of Buck Converter | 3.3V |

TABLE XIV: shows the voltage levels at the different stages of power conversion.

## V. CONCLUSION

This paper focused on the power electronic converter types, ways the circuits can be improved with their advantages and disadvantages and their voltage waveforms at each conversion stage. In non-resonant coupled systems, typical example being transformers, power can be transferred within a very short range and there is usually the need for a magnetic core. Thus, for longer distance applications, they are highly inefficient. In this paper, the fundamental resonance circuits were discussed and specifically for the purpose of this study, the series-series (SS) compensation was employed.

## REFERENCES

[1] P. S. Huynh, D. Ronanki, D. Vincent, and S. S. Williamson, "Overview and comparative assessment of single-phase power converter topologies of inductive wireless charging systems," *Energies*, vol. 13, no. 9, p. 2150, 2020.

[2] K. N. Mude, "Wireless power transfer for electric vehicle," 2015.

[3] M. Al-Saadi, A. Ibrahim, A. Al-Omari, A. Al-Gizi, and A. Craciunescu, "Analysis and comparison of resonance topologies in 6.6 kw inductive wireless charging for electric vehicles batteries," *Procedia Manufacturing*, vol. 32, pp. 426–433, 2019.

[4] F. Pellitteri, N. Campagna, V. Castiglia, A. Damiano, and R. Miceli, "Design, implementation and experimental results of an inductive power transfer system for electric bicycle wireless charging," *IET Renewable Power Generation*, vol. 14, no. 15, pp. 2908–2915, 2020.

[5] S.-Y. Cho, I.-O. Lee, S. Moon, G.-W. Moon, B.-C. Kim, and K. Y. Kim, "Series-series compensated wireless power transfer at two different resonant frequencies," in *2013 IEEE ECCE Asia Downunder*. IEEE, 2013, pp. 1052–1058.